Characterization of cermet coatings deposited by low-pressure cold spraying

M. Winnicki, A. Malachowska, M. Rutkowska-Gorczyca, P. Sokolowski, A. Ambroziak, L. Pawlowski

Characterization of cermet coatings deposited by low-pressure cold spraying

M. Winnicki[a], A.Małachowsk[a,b], M. Rutkowska-Gorczyca[a],
P.Sokołowski[a,b], A.Ambroziak[a], L.Pawłowski[b]

[a]Wrocław University of Technology, Wyb. Wyspiańskiego 27, Pl-50371 Wroclaw, Poland
[b]SPCTS, University of Limoges, UMR CNRS 7315, 12 Rue Atlantis, F-87068 Limoges, France

The paper presents the influence of substrate preparation on low pressure cold sprayed (LPCS) coatings adhesion strength and microhardness. The LPCS process parameters such as: (i) gas temperature; (ii) gas pressure;(iii) gun linear speed; (iv) powder feeding rate; and (v) spray distance were kept constant during deposition. The coatings were sprayed using metallic powders having different morphology, namely spherical (Al, Zn, Sn, Cu) and dendritic (Ni, Cu) with the grain size of about $-50 + 10$ μm. These powders were mixed with alumina before spraying in a weight ratio of 50:50. Copper and aluminium alloy were used as substrates. The substrate preparation included sand-blasting and grinding. The coating microstructures were characterized by scanning electron microscopy (SEM) and X-ray diffractometry (XRD). The adhesion strengths of coatings were determined by pull-off method and showed that coating adhesion reached 65 MPa. The measurements of coatings micro-hardness were carried out also. Finally, the values of adhesion strength and microhardness of coatings were correlated with the substrate preparation and the microstructure of coatings. The microhardness of LPCS coatings was in the range of 20 to 201 HV0.02 and depended mostly on sprayed powder material.

1. Introduction

In the cold spray method the powder particles get accelerated in the stream of compressed gas (air, nitrogen or helium) and subsequently impact a substrate. The gas is flowing in de Laval nozzle having special convergent–divergent shape. When the value of critical velocity is reached, the particles start to adhere to the substrate [1,2]. Two varieties of the method can be distinguished: (i) low-pressure and (ii) high-pressure cold spraying. In the low-pressure cold spraying (LPCS) method air or nitrogen is usually used as working gases with the pressure not exceeding 0.9 MPa and temperature up to 650 °C [2].

The adhesion strength and hardness are the most important mechanical properties in cold spraying. There is no metallurgical bonding between particles and substrate because powder particles are solid at deposition. The bonding is realized thanks to the local deformation of the material at the interface, as the powder particles strike the substrate. As a result of high strain-rate deformation of materials the adiabatic shear bands are formed. Subsequently oxides are removed from the surfaces of powders and substrate by the forming of the plastic metal jet and the metallically pure surfaces can come into contact [3,4]. Besides mechanical bonding mechanism, the other ones, such as e.g. the local metallurgical one was reported by Hussain [5] and by Guetta [6]. Such process parameters as the substrate preparation, operational spray parameters, and heat treatment of substrate prior to deposition and the deposited coatings may influence adhesion.

An important factor affecting the coatings' adhesion and hardness of cold sprayed coatings is the fraction of ceramic in a cermet powder. The addition of ceramics may act in a following way: (i) preventing of nozzle clogging; (ii), activating of the metallic surfaces by removing oxides; and, (iii) hardening of metal co-particles by tamping effect. Hence, an increase of the fraction of ceramics in cermet powder may, to a degree, improve the adhesion of the coating [2,7–15].

The adhesion values of low-pressure cold sprayed cermet coatings were reported in the literature to be as high as 60 MPa or even more [2,7–13]. The most commonly analysed cermet materials were: copper, aluminium and nickel with addition of Al_2O_3.

The presented research was carried out to check the influence of substrate preparation on mechanical properties of various types of cold sprayed coatings. The cold sprayed copper and nickel coatings can be used as electrical conductors. Aluminium, zinc and nickel can be deposited as the anticorrosive coatings. Moreover aluminium–alumina powder mixture is commonly used to regenerate defects in aluminium, steel or cast iron products. Tin coatings can be deposited on the contact surface of current connectors as an electrochemical corrosion protection coating.

* Corresponding author. Tel./fax: +48 713202735.
E-mail address: marcin.winnicki@pwr.wroc.pl (M. Winnicki).

2. Materials and methods

2.1. Powders and substrates preparation

Commercially available powders of the following metals: tin (T2-00-05), zinc (K-00-11), aluminium (K-10-01), copper electrolytic (E-copperK-01-01), nickel (K-32) from Obninsk Center for Powder Spraying (Obninsk, Russia) and copper spherical (S-copper) from Sentes Bir, (Ankara, Turkey), were used in the spraying process. The granulometry tests (Analysette 22 MicroTec plus, Fritsch, Markt Einersheim) showed that the size of particles was in the range of $-50 + 10$ μm. Each powder was mixed with Al_2O_3 in weight ratio 50:50 before deposition (Obninsk Center for Powder Spraying, Obninsk, Russia). The morphology of the selected powders is shown in Fig. 1 (dark particles are Al_2O_3). The tin, zinc, S-copper and aluminium powders were produced by gas atomizing and were spherical. E-Copper and nickel powders were produced by electrolytic method and the particles were dendritic. The Al_2O_3 powder was prepared by crushing and its particles had an irregular shape.

The substrate materials were 7 mm thick discs having a diameter of 40 mm of copper M1E and aluminium alloy AA1350 with following chemical composition (wt.%): 0.12% Si, 0.24% Fe, 0.02% Cu, 0.01% Mn, 0.01% Cr, 0.07% Zn, 0.02% Ti and Al bal. The substrates surface was activated by sand blasting under a pressure of 0.6 MPa using alumina sand (mesh 45) or ground with SiC abrasive paper (mesh 1000). The aluminium alloy substrate AA1350 reached after grinding and sand-blasting surface roughness of $R_a = 0.36$ μm and $R_a = 6.45$ μm, respectively. The copper substrate the surface roughness were equal to $R_a = 0.33$ μm and $R_a = 5.27$ μm, respectively. The roughness was measured using Form Talysurf 120L profilometer (Taylor-Hobson, Leicester, UK).

2.2. Design of spray process experiments

The coatings were sprayed using a DYMET 413 (Obninsk Center for Powder Spraying, Obninsk, Russia) set up. The setup includes a heater and the de Laval nozzle with a circular outlet having an internal diameter of 5 mm. The process parameters such as: (i) gas temperature; (ii) gas pressure; (iii) gun linear speed; (iv) powder feeding rate; and (v) spray distance were kept constant during deposition (see Table 1). Air was used as the working gas and the distance between next spraying gun passes relative to the substrates was 3.7 mm. The process parameters collected in Table 1 were found to be optimal in respect of spraying efficiency for each powder.

2.3. Microstructure characterization

The metallographic examinations of powders and coatings were carried out using a SEM microscope with secondary electrons detector (Phenom G2 pro, Eindhoven, The Netherlands). The micrographs were made on the coating cross-section. The metallographic cross-section had been etched in accordance with Polish standard PN-75/H-04512 before examination, depending on the coating material: Sn coating with 1% NaCl; Zn with Nital; Al with 10% HF; Cu with $(NH_4)_2S_2O$ and Ni with 65% HNO_3. The phase analysis of coatings was made with X-ray diffractometer (D8 Advance, Bruker) using CuKα1 radiation in the range of 2θ angles from 20° to 100°. Diffrac + Eva software was used to identify phases in the coating microstructure. Furthermore semi-quantitative analysis was prepared to check the proportion of metallic powder and Al_2O_3 in the deposited coatings.

2.4. Adhesion strength

The adhesion tests were made following the standard PN-EN 582 [16]. The samples were hot bonded using epoxy resin Epidian 100 with an average strength of 70 MPa. In the case of tin coatings, cold-setting adhesive DISTAL with an average strength of 48 MPa was used. Three tests were carried out for each experimental run and the average adhesion value was determined. The tests were carried out for a constant coating thickness of 500 μm. The coatings deposited from the spherical Sn, Zn, S–Cu and Al powders were faced by turning. The coatings made of the dendritic E–Cu and Ni powders, were submitted to the tensile pull test as-sprayed. The following types of the failure at adhesion test were recognized: (i) adhesive—when the fracture occurred at the substrate/coating interface (A); (ii) adhesive–cohesive—the fracture occurred non-uniformly on the entire cross section (A/C); (iii) cohesive—when the fracture occurred within the coating (C); and (iv) failure in the epoxy resin (ER).

2.5. Microhardness measurements

Microhardness was measured following the standard PN-EN ISO 6507-3:2007P with the use of a Digital micro Hardness Tester MMT-X7 MATSUZAWA CO., LTD (Akita, Japan). Three different forces (1.961, 4.903, and 9.807 N) were chosen for each type of coating to eliminate the errors resulting from the heterogeneous composition of cermets. Microhardness was given as an average of five measurements in the middle of coating. However it is necessary to remember that the microhardness results cannot be compared directly because of different force values used in measurements.

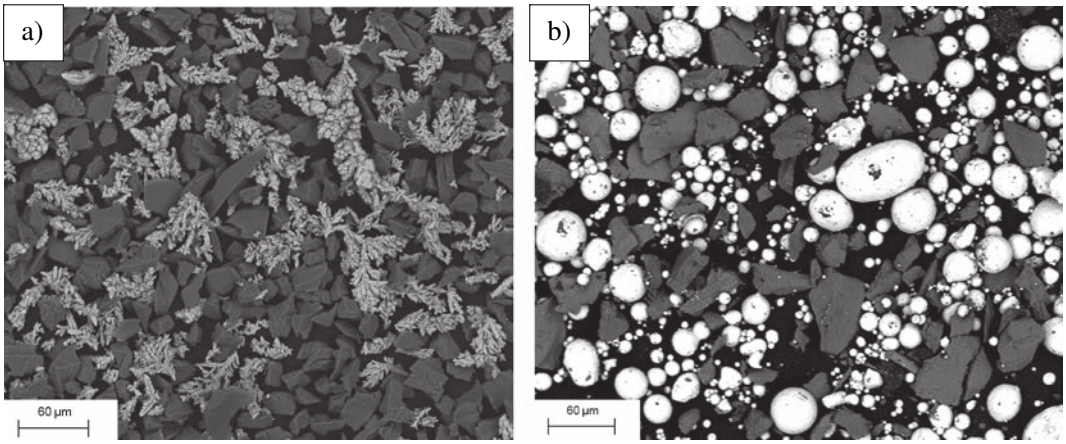

Fig. 1. SEM (secondary electrons) micrographs of example powders used to spray: E–Cu + Al_2O_3 (a) and S–Cu + Al_2O_3 (b).

Table 1
Spray parameters and coatings thickness.

	Spraying parameter							Thickness of coatings [μm]
	Powder	No. of coating runs	Working gas preheating t emperature [°C]	Gas pressure [MPa]	Linear speed [mm/s]	Powder feed rate [g/min]	Spray distance [mm]	
Value	Sn + Al_2O_3	3	200	0.5	10	40	20	500–660
	Zn + Al_2O_3	2	400	0.7				550–870
	Al + Al_2O_3	2						520–760
	E–Cu + Al_2O_3	2						510–720
	Ni + Al_2O_3	3						480–640
	S–Cu + Al_2O_3	4	600	0.9				440–580

3. Results

3.1. Coating microstructure

The micrographs of LPCS coatings are presented in Figs. 2–4. The coatings deposited using spherical powders (Sn, Zn, Al, S–Cu) showed the microstructures with larger amount of alumina than that deposited from the dendritic powders (E–Cu, Ni).

The tin particles deform plastically and form dense coatings without apparent porosity. The regions more remote from the substrate, where larger particles occurred, were subject to much weaker deformation.

Despite high temperature of working gas (400 °C) used in the process, the zinc and aluminium coatings did not show any oxidation. Using an addition of alumina during spray process allowed obtaining coatings with a high density and minimized the presence of pores. But at the same time the particles of alumina created some regions of concentrations extended in the zinc coating along the thickness of about 50 μm from the substrate (Fig. 2, discussed regions labelled with lines). The same was observed in the case of aluminium coating.

Spherical copper was deposited with highest temperature and pressure, 600 °C and 0.9 MPa, respectively. Nevertheless four runs were needed to build 500 μm thick coating what corresponded to the lowest spraying efficiency of compared powders. The coatings built up of spherical powders, were generally dense and free of pores (Fig. 3). The regions with a high concentration of brittle alumina powder could be also observed in the coating microstructure (labelled with lines).

Despite the dendritic form of copper powder, the E–Cu + Al_2O_3 cermet coating had a microstructure free of pores (Fig. 4a). One can notice that a large amount of fine alumina particles are present between the individual copper particles. The concentration of alumina may lead to the formation of the brittle regions in the coatings. Such regions were found in the coating deposited on the ground substrate (Fig. 4b).

Fig. 5 shows the Ni + Al_2O_3 coating. Its microstructure was the most heterogeneous among all the examined samples. Also the amount of alumina visible in the coating microstructure was the smallest in comparison with the other coatings and a considerable amount of pores occurred at the particle boundaries. Additionally local microcracks were discovered in the nickel coatings.

The phase analysis made by X-ray diffraction did not show any oxidation of metallic powders at spraying. The coating microstructures consisted of only two phases: of pure metal and of corundum (see Fig. 6). Moreover, the semi-quantitative analysis of coatings enabled to find out that the deposition process changed the fraction of the alumina to the metal in cermet with regard to the initial one. Consequently, the coatings had the amount of alumina ranging from 14 to 30 wt.% (depending on coatings).

3.2. Adhesion strength

The samples after the adhesion tests are shown in Fig. 7. It was visible that in the Al + Al_2O_3 and E–Cu + Al_2O_3 samples the fracture occurred at the interface to substrate (indicated by arrows). It was possible to notice also some parallel lines on the surface of Al + Al_2O_3 and Ni + Al_2O_3 coatings after adhesion tests which corresponded to the next passes of spraying gun during deposition process. Generally Al + Al_2O_3 coatings were characterized by adhesive type of fracture and

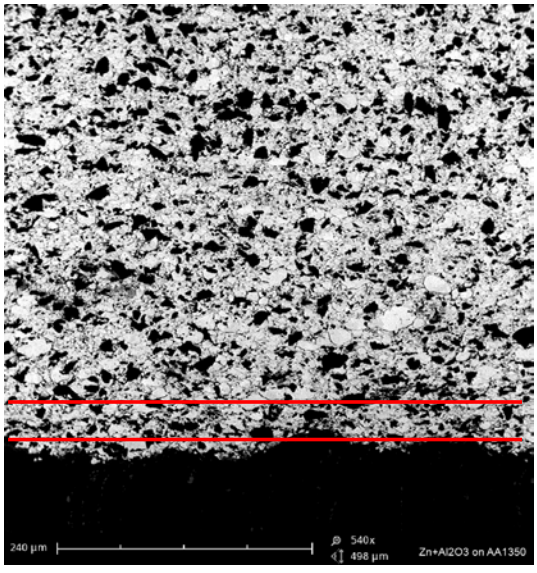

Fig. 2. SEM (secondary electrons) micrographs of cold sprayed Zn + Al_2O_3 coating on sand-blasted AA1350 substrate.

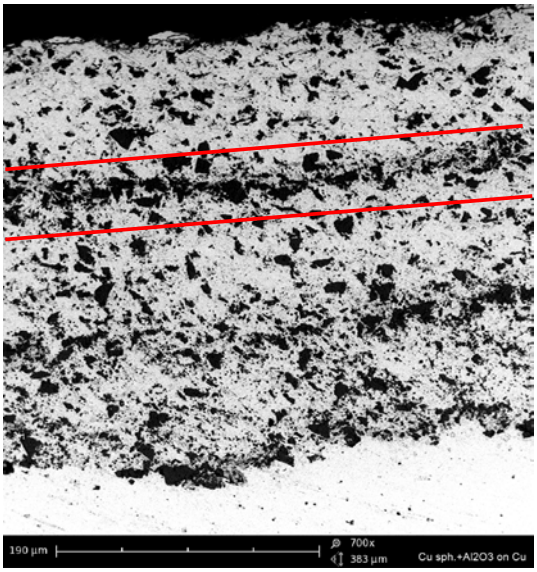

Fig. 3. SEM (secondary electrons) micrographs of cold sprayed S–Cu + Al_2O_3.

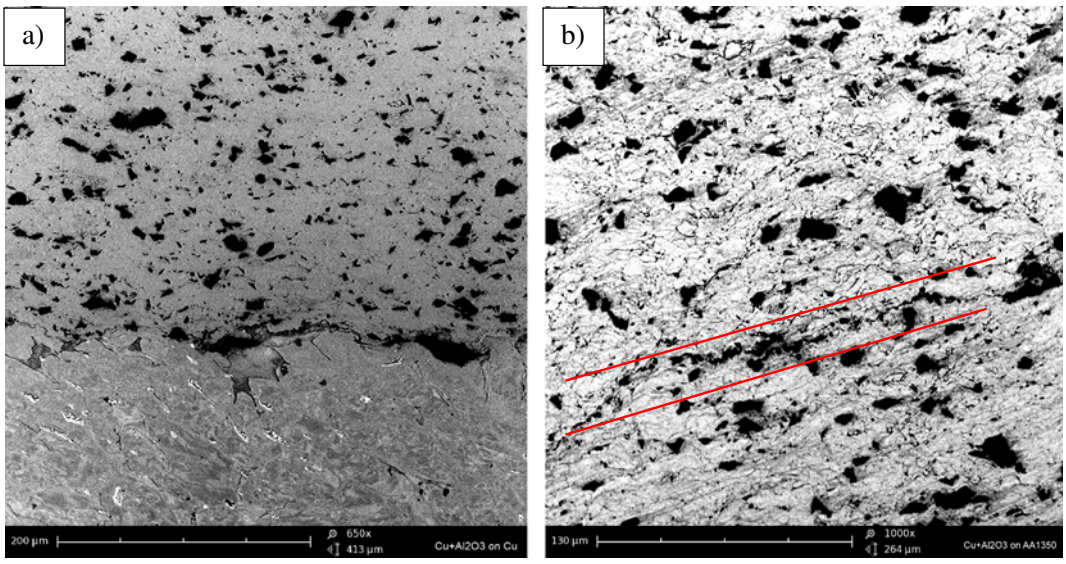

Fig. 4. SEM (secondary electrons) micrographs of cold sprayed E–Cu + Al_2O_3 coatings on sand-blasted Cu substrate (a) and brittle alumina phase concentration inside the coating deposited onto ground AA1350 substrate (b).

E–Cu + Al_2O_3 coatings by adhesive–cohesive type. In the case of cermets of Al_2O_3 with Ni, Sn and S–Cu a cohesive-type fracture occurred inside the coating. Finally, the adhesion tests of Zn + Al_2O_3 coatings had the fracture in the epoxy resin. Moreover, the way of the surface activation was very important. The alumina particles do not adhere to the metallic substrate having ground surface at cold spraying. This weakens the adhesion of cermet coating to such substrates. This may explain the adhesive failure of cermets of Al_2O_3 with Sn, Ni and E–Cu deposited onto the ground substrate.

The adhesion strength test results are shown in Table 2. The cermets sprayed using metallic powders having spherical shape i.e. Al, Zn, S–Cu and Sn were characterized by much greater adhesion strength than that sprayed using the dendritic ones (E–Cu and Ni). It is clearly seen when comparing their adhesion strength with that of the cermets including copper S–Cu and E–Cu. Consequently, the cermets sprayed using S–Cu powder resulted in coatings with adhesion strength of 36 MPa (while dendritic E–Cu powder to 25 MPa only (see lines 15 and 19 of Table 2). The substrate preparation and substrate material do not play a significant role in the adhesion of the coating while spraying the cermets with spherical metallic powders. On the other hand, the use of dendritic powders as metals in cermets resulted in the coatings having adhesion strongly depending on the substrate preparation method. The sand-blasting was the most efficient substrate preparation method and gave the resulting coatings with the greatest adhesion strength. The adhesion strength of 57 MPa (see line 11 in Table 2) was found for the Al + Al_2O_3 coating sprayed onto the sand-blasted Cu substrate and the lowest one of 2 MPa (line 18, Table 2) was found for the Ni + Al_2O_3 coating deposited on the ground aluminium substrate.

In the case of zinc coatings, the test was not successful and the failure occurred in the adhesive (5, 7 and 8). It must be underlined that the samples including Zn were bound with epoxy resin without heating. Consequently, the adhesion strength of this epoxy is lower than that of epoxy prepared with heating.

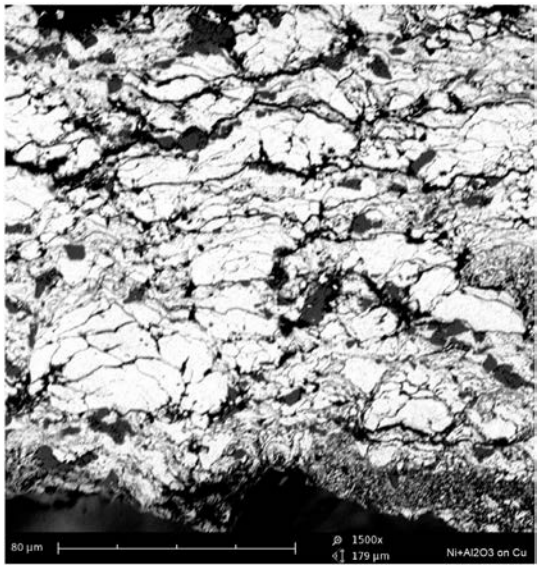

Fig. 5. SEM microstructure (secondary electrons) of cold sprayed Ni + Al_2O_3 coating on sand-blasted Cu substrate.

3.3. Microhardness

The measured microhardness values of the LPCS coatings for the particular materials are shown in Table 2. The measurements were performed for both powders and sprayed coatings and then compared. The microhardnesses of LPCS cermets are higher than the microhardnesses of their metallic matrix. Consequently, the microhardness of the Sn + Al_2O_3 coatings was the lowest and estimated to be about 20 +/− 1 HV0.2 comparing with the microhardness of metal matrix powder of 9 +/− 3 HV0.01. The mean microhardness of the Zn + Al_2O_3 coating were about 57 HV0.2 and 56 HV1.0 comparing with microhardness of metal matrix powder equal to 28 +/− 6 HV0.01. The coating of Al + Al_2O_3 had hardness of 90 HV0.2 and 75 HV1.0 comparing with the hardness of metal matrix powder equal to 31 +/− 8 HV0.01.

The cermet of S–Cu + Al_2O_3 had microhardness of 201.1 HV0.2 and 186.7 HV1.0 while spraying on aluminium substrate comparing 86 +/− 3 HV0.01 for metal matrix powder. The values of 182.5 HV0.2 and 173.8 HV1.0 were found for S–Cu + Al_2O_3 deposited onto copper substrates. The microhardness of E–Cu + Al_2O_3 was about 119 HV0.2 and 90 HV1.0 while spraying onto the AA1350 substrate and 126.2 HV0.2 and 119 HV1.0 onto the Cu substrate. For comparison, the microhardness of metal matrix powder was about 72 +/− 10 HV0.01. Finally, the Ni + Al_2O_3 coating microhardness was in the range of 165 to 178 HV0.2 and 170 HV1.0. The microhardness of metal matrix powder was about 150 +/− 5 HV0.01.

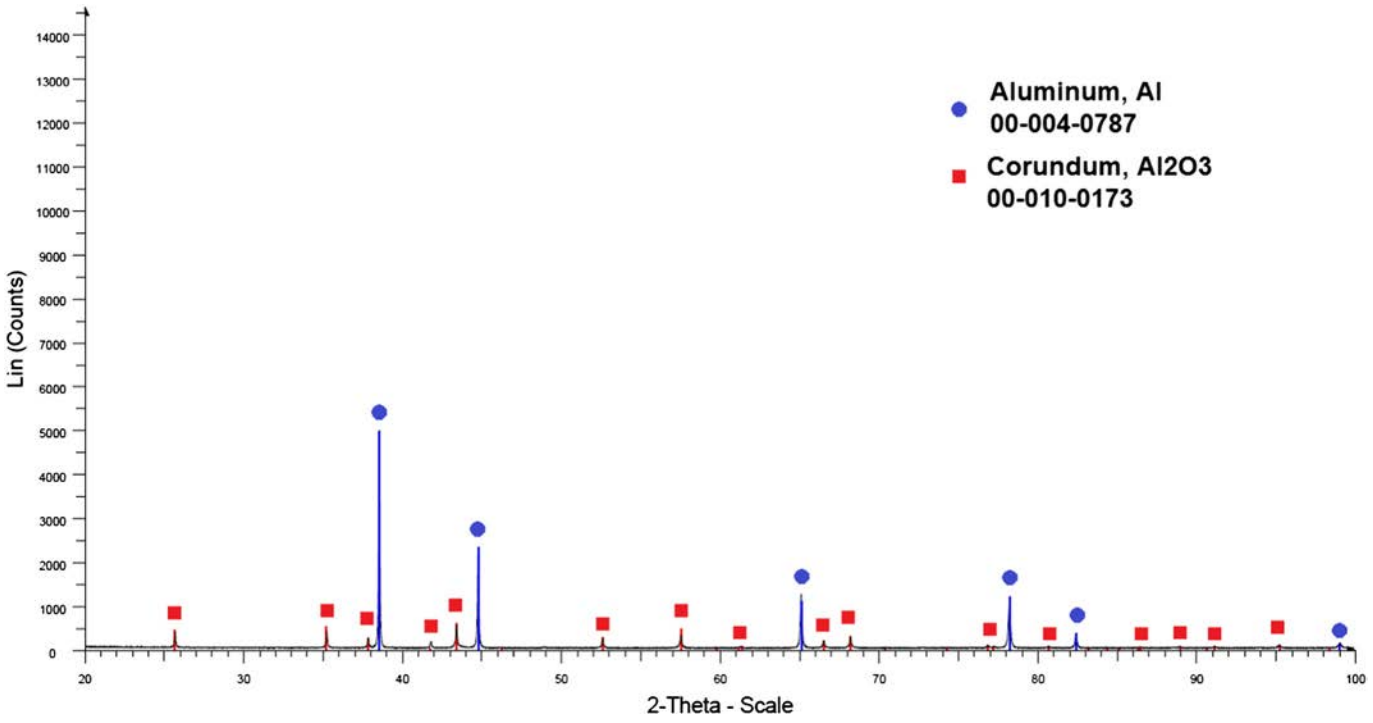

Fig. 6. Phase analysis of cermet coating made by X-ray diffraction (Al + Al_2O_3 coating).

4. Discussion

The addition of alumina to different metallic powders allowed obtaining of cold sprayed coatings characterized by low porosity. The adhesion strengths of sprayed cermets were satisfactory. The presence of alumina increased considerably the microhardness of the metal particles in the coatings [2,9]. The hardening of metal particles by alumina occurred at spraying. This effect resulted also in the reduction of pores

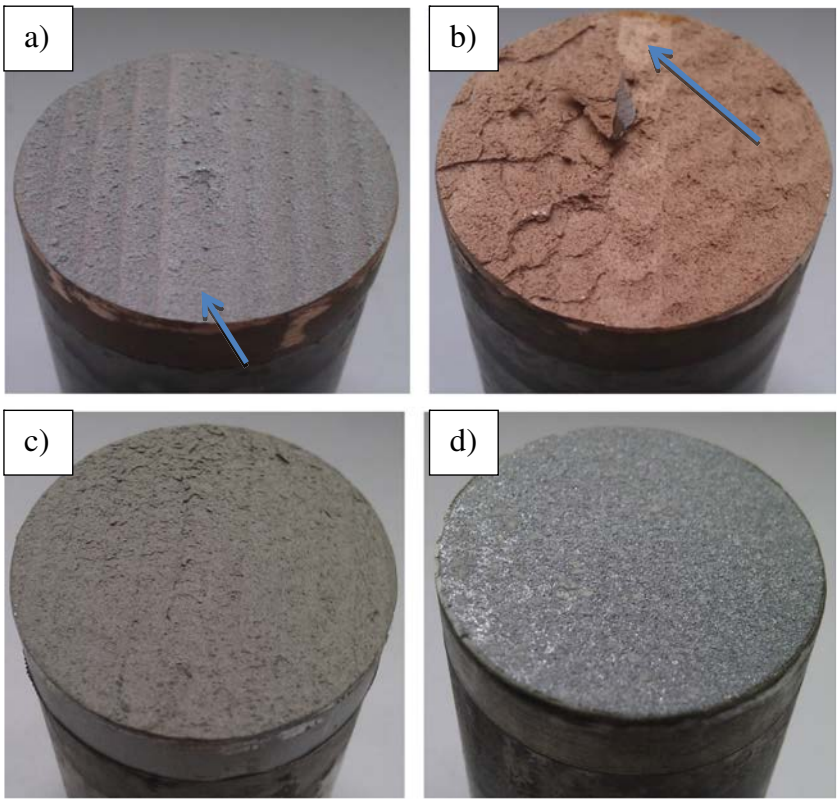

Fig. 7. The types of fractures after pull off tests: a) adhesive-type failure of Al + Al_2O_3 coating deposited initially on Cu substrate, b) adhesive–cohesive failure of E–Cu + Al_2O_3 coating deposited on Cu substrate, c) cohesive-type failure of Ni + Al_2O_3 coating on AA1350 substrate, and d) failure in epoxy resin of Zn + Al_2O_3 coating deposited onto AA1350 substrate.

Table 2
Microhardness and adhesion strength of sprayed coatings.

Exp. no.	Powder material	Subst. mater.	Subst. prepar.	Hardness						Adhesion strength [MPa]	SD	Type of fracture
				HV0.2		HV0.5		HV1.0				
				Coating		Coating		Coating				
				AV	SD	AV	SD	AV	SD			
1	Sn + Al_2O_3	Al	SB	19.5	0.86	16.8	0.05	16.5	0.25	34	0.74	C
2			G	–	–	–	–	–	–	33	0.16	A
3		Cu	SB	–	–	–	–	–	–	31	1.97	C
4			G	19.8	0.90	16.3	0.41	16.6	0.21	30	2.39	A
5	Zn + Al_2O_3	Al	SB	55.9	0.96	58.3	0.50	56.2	0.85	55	–	ER
6			G	–	–	–	–	–	–	52	3.13	A
7		Cu	SB	–	–	–	–	–	–	43	–	ER
8			G	57.3	1.08	56.6	0.45	56.4	0.83	43	–	ER
9	Al + Al_2O_3	Al	SB	–	–	–	–	–	–	55	1.44	A
10			G	–	–	–	–	–	–	55	2.84	A
11		Cu	SB	90.1	4.08	77.5	0.90	77.1	0.54	57	1.78	A
12			G	90.8	5.13	80.8	1.05	73.5	2.02	52	2.57	A
13	E–Cu + Al_2O_3	Al	SB	–	–	–	–	–	–	24	1.19	A/C
14			G	119.4	1.71	96.9	3.46	89.7	2.91	15	1.69	A
15		Cu	SB	126.2	5.01	120.6	4.27	118.6	1.52	25	1.38	A/C
16			G	–	–	–	–	–	–	16	1.40	A
17	S–Cu + Al_2O_3	Al	SB	–	–	–	–	–	–	35	1.13	C
18			G	201.1	7.39	192.2	2.65	186.7	0.85	30	1.36	C
19		Cu	SB	182.5	6.85	179.8	4.47	173.8	5.08	36	1.39	C
20			G	–	–	–	–	–	–	33	1.95	C
21	Ni + Al_2O_3	Al	SB	–	–	–	–	–	–	6	0.18	C
22			G	165.3	31.08	173.9	11.36	169.7	8.01	2	0.14	A
23		Cu	SB	177.7	13.85	170.9	11.94	169.8	4.56	7	0.66	C
24			G	–	–	–	–	–	–	4	0.59	A

SB—sand-blasted, G—grinded, AV—average value, and SD—standard deviation.
A—adhesive type of fracture, A/C—adhesive-cohesive type of fracture,C—cohesive type of fracture; and ER—fracture in the epoxy resin.

and filling of voids in coating [11–13]. On the other hand, the formation of alumina concentrations resulted in the formation of brittle regions in the coating. These regions were characterized by a formation of cracks in the deposits. Consequently, the type of fracture during pull-off tests and the adhesion strengths were strongly correlated to the microstructure of prepared coatings, what was also observed by other authors [2,10].

The tin coatings showed cohesive-type of fracture at the pull-off tests. This resulted from the microstructural heterogeneity of the coatings. The zone close to the substrate contains tin particles hardened by alumina particles at spraying. The zone in the mid-coating contains larger and less deformed particles. Consequently, a cohesive-type fracture occurred. The composite coatings including Al_2O_3 reinforcement with spherical Zn and Al powders had fine alumina particles concentrated close to the interface with the substrate. As Wand et al. described before [10], the pull-off tests indicated the adhesive type of failure, due probably to the presence of these brittle concentrations.

The microstructure of S–Cu + Al_2O_3 coatings showed similar alumina concentrations, which separated single spraying runs. Their presence may be explained by the fact that alumina having high velocity strikes the substrate or previously deposited coating and remains attached. The upper part of the coating showed some pores (Fig. 3). The porosity might be related to the copper particles, which did not deform sufficiently to fill all voids present in the coating.

The E–Cu + Al_2O_3 coatings were characterized by fine alumina particles deposited between the copper grains forming again some concentrations. Their presence could have led to the formation of brittle regions in the coating and to the adhesive-cohesive type of fracture.

The addition of ceramic to copper metal powders increased significantly the mechanical properties of the coatings. According to the previous research [17], the adhesion of pure E–Cu and S–Cu coatings amounted to 10 ± 1 MPa and to 28 ± 1 MPa respectively, while deposited onto aluminium substrate. Presented research showed that copper–alumina mixture had higher adhesion strength resulting to 24 MPa for E–Cu + Al_2O_3 and 35 MPa for S–Cu + Al_2O_3. At the same time S–Cu coating had a microhardness of about 137 HV0.2 while with alumina admixture it was increased to 201.1 HV0.2. However the microhardness of coatings deposited with dendritic copper powder with and without alumina admixture showed similar values. The microhardness of E–Cu was about 120 HV0.2 what was comparable to 119 HV0.2 obtained for E–Cu + Al_2O_3 coating.

The nickel coatings had a very heterogeneous structure. The kinetic energy of particles at impact was too low to deform them and to reduce the voids. Consequently, the Ni + Al_2O_3 coatings were more porous than the other ones. Similarly, the adhesion strength was the smallest measured confirming the observations made by other authors [2]. The cohesive-type failure occurred in these coatings. The fracture at the pull-off test propagated along the weakly bound particle boundaries. The small deformation of nickel particles at spraying as well as their high hardness could have resulted in rebounding of alumina particles during processing, what was also reported in [13]. That is why the lowest quantity of alumina reinforcement could be observed in Ni + Al_2O_3 cermet coatings (Fig. 5).

The mechanical properties of the coatings depended also on the substrate preparation. The substrates prepared by grinding were struck by alumina particles, which moved faster in the spraying stream than metal particles. The particles removed occurring oxide layers. Small particles could not result in a significant roughening of the substrate. Therefore, the bonding between metal particles and the substrate was relatively weak and adhesion strength of the sprayed coatings was small.

As tin, zinc, aluminium and S-copper powders deformed at spraying uniformly, contrarily to E-copper and to nickel powders. It aroused from irregular shape and size of dendritic particles. As a result coatings with higher porosity were obtained. Such observation was also made by other authors [2,18,19]. One of the consequences of this effect is the fact that the dendritic powders showed strong dependence of microhardness on load at testing and important dispersion of measured values. The nickel coatings had an exceptionally heterogeneous structure. In their case, the process energy was too low in order for the

deformed particles to fill the space between the individual particles. As a result, the Ni + Al_2O_3 coating was more porous than the other coatings and showed highest dispersion of microhardness values.

5. Conclusions

This study presented in the paper focussed on the analysis of the effect of substrate preparation and of type of metallic powder on the adhesion strength of cermet coatings deposited by low pressure cold spraying. SEM microscopy was used to analyse the microstructure of coatings and showed that the coatings were characterized by relatively low porosity. X-ray diffraction investigations revealed that the metallic matrix of coatings was only slightly oxidized and the coatings included mainly two phases: pure metal and alumina. Furthermore, the sprayed coatings showed much smaller quantity of alumina than the initial feedstock powders. It can be concluded that the important part of alumina rebounded at processing and was not included in the coating.

The pull-off tests showed an effect of initial metallic powder type on the adhesion strength. The coatings deposited from spherical powders were characterized by higher adhesion strength than that produced from the dendritic ones. This effect was proved, in particular, for copper coatings deposited using spherical and dendritic powders. Processing the spherical powders results in coatings which adhere well to the substrate independently on substrate material or substrate preparation. The coatings sprayed using dendritic powders had to be optimized and sand-blasting of substrate was found to be the best way to obtain a strong coating adhesion.

As expected, the use of the cold sprayed cermets of metal with alumina reinforcement enabled to obtain the coatings having microhardness much greater than that of initial metallic powder.

Acknowledgements

This paper is based on research funded by the National Science Centre as part of project no. 2011/01/N/ST8/04975 entitled: "Adhesive properties of various material coatings deposited by low-pressure cold spraying".

References

[1] T. Schmidt, F. Gärtner, H. Assadi, H. Kreye, Acta Mater. 54 (2006) 729–742.
[2] H. Koivuluoto, J. Lagerbom, M. Kylmalahti, P. Vuoristo, J. Therm. Spray Technol. 17 (5-6) (2008) 721–727.
[3] H. Assadi, F. Gärtner, T. Stoltenhoff, H. Kreye, Acta Mater. 51 (2003) 4379–4394.
[4] M. Grujicic, C.L. Zhao, W.S. DeRosset, D. Helfritch, Mater. Des. 25 (2004) 681–688.
[5] T. Hussain, D. McCartney, P. Shipway, D. Zhang, J. Therm. Spray Technol. 18 (3) (2009) 364–379.
[6] S. Guetta, M. Berger, F. Borit, V. Guipont, M. Jeandin, M. Boustie, Y. Ichikawa, K. Sakaguchi, K. Ogawa, J. Therm. Spray Technol. 18 (3) (2009) 331–342.
[7] H. Mäkinen, J. Lagerbom, P. Vuoristo, Thermal Spray 2007: Global Coating Solutions: Proceedings of the 2007 International Thermal Spray Technology, Beijng, China, 2007.
[8] X.-J. Ning, J.-H. Kim, H.-J. Kim, C. Lee, Appl. Surf. Sci. 255 (2009) 3933–3939.
[9] H. Koivuluoto, P. Vuoristo, J. Therm. Spray Technol. 19 (5) (2010) 1081–1092.
[10] Q. Wang, K. Spencer, N. Birbilis, M.-X. Zhang, Surf. Coat. Technol. 205 (2010) 50–56.
[11] K. Spencer, D.M. Fabijanic, M.-X. Zhang, Surf. Coat. Technol. 204 (2009) 336–344.
[12] E. Irissou, J.G. Legoux, B. Arsenault, Ch. Moreau, J. Therm. Spray Technol. 16 (5-6) (2007) 661–668.
[13] H. Koivuluoto, P. Vuoristo, J. Therm. Spray Technol. 18 (4) (2009) 555–562.
[14] L. Pawłowski, The Science and Engineering of Thermal Spray Coatings, John Wiley & Sons Ltd, Chichester, 2008.
[15] R.G. Maev, V. Leshchynsky, Introduction to Low Pressure Gas Dynamic Spray, WILEY-VCH Verlag GmbH & Co, Weinheim, KGaA, 2008.
[16] Standard: Thermal spraying, Determination of Tensile Adhesive Strength, PN-EN 582, Polish Standards Association, Poland, 1996.
[17] M. Winnicki, A. Małachowska, M. Rutkowska-Gorczyca, A. Ambroziak, Prz. Spawal. 2 (2014) 47–52 (in Polish).
[18] H. Koivuluoto, P. Vuoristo, J. Therm. Spray Technol. 19 (5) (2010) 1081–1092.
[19] K.J. Hodder, H. Izadi, A.G. McDonald, A.P. Gerlich, Mater. Sci. Eng. A 556 (2012) 114–121.